ce/papers
The online collection for conference papers in civil engineering
Ernst & Sohn A Wiley Brand

ORIGINAL ARTICLE

SDSS 2022
The International Colloquium on Stability and Ductility of Steel Structures
14-16 September, University of Aveiro, Portugal
Ernst & Sohn A Wiley Brand

Seismic Fragility Curves of Steel Frames Equipped with Easily Repairable Dissipative Devices

Giulia Giuliani[1], Roberto Andreotti[1], Nicola Tondini[1], Oreste S. Bursi[1]

Correspondence

Prof. Nicola Tondini
University of Trento
Department of Civil, Environmental and Mechanical Engineering,
via Mesiano 77,
38123 Trento, Italy
Email: nicola.tondini@unitn.it

Abstract

This paper provides insight into a probabilistic demand analysis of a steel-concrete structures equipped with novel dissipative components. DISSIPABLE components were studied in the framework of a European Research Fund for Coal and Steel (RFCS) project, funded to test large-scale structures in which the dissipation is concentrated in specifically designed elements that act like a fuse and can easily be replaced after a seismic event. Incremental Dynamic Analyses (IDAs) were performed to investigate the influence of equipping steel frames with two different dissipative seismic devices, namely the Dissipative Replaceable Beam Splice (DRBeS) and the Dissipative Replaceable Link Frame (DRLF). The benchmark models were calibrated on the results of laboratory full-scale tests, carried out in the project framework. In addition, the DISSIPABLE frame behaviour was compared with a state-of-the-art moment-resisting frame, designed according to the capacity design philosophy. Probabilistic demand models were developed, and seismic fragility curves were then derived to compare the behaviour of the analysed structural systems.

Keywords

Seismic performance; incremental dynamic analysis; fragility curves; full-scale tests; steel structures; seismic devices; resilient structures.

1 Introduction

Structural systems characterised by low-damage when subjected to seismic actions are particularly sought to minimise the loss of functionality after a major seismic event. In this respect, the European Research Fund for Coal and Steel (RFCS) project DISSIPABLE was funded to test large-scale structures in which the dissipation is concentrated in specifically-designed components that act like fuses during a seismic event and can easily be replaced after it.

In recent years, the probabilistic Performance-Based Earthquake Engineering (PBEE) methodology has become popular, and an increasing number of seismic fragility functions for a particular structural typology or component, crucial for both risk assessment and/or a probabilistic PBEE application, are being developed for both civil [1] and industrial buildings [2][3]. On these premises, in this paper Incremental Dynamic Analyses (IDAs) were applied to investigate the influence of equipping steel frames with two different dissipative seismic devices analysed in DISSIPABLE, namely the Dissipative Replaceable Beam Splice (DRBeS) and the Dissipative Replaceable Link Frame (DRLF).

In particular, the frame behaviour equipped with DRBeS and DRLF was compared with a state-of-the-art moment-resisting frame, designed according to the capacity design philosophy. The frame has the same geometry as the DISSIPABLE structures, so that differences in the behaviour can be highlighted under the same design conditions. The three different frames were designed and modelled respectively with the finite element software SAP2000 [4] and OpenSees [5]. With the purpose of having high-fidelity models for comparing the behaviour of the frames equipped with the devices and the state-of-the-art structure, the benchmark models were calibrated on the results of laboratory full-scale tests, carried out in the framework of the DISSIPABLE project.

IDAs were performed monitoring the maximum interstorey drift and the rotation of the dissipative region of the structures. Finally, probabilistic demand models were developed, and seismic fragility curves were derived to compare the behaviour of the analysed structural systems.

The paper is organised as follows: in Section 2 the details of fragility methods and the description of the ground motion selection are given; in Section 3 are reported the numerical models of the building prototypes; whilst the description of the IDAs results as well as the fragility curves are presented in Section 4; in Section 5 a comparison of the behaviour of the structure is illustrated and finally in Section 6 conclusive remarks are drawn.

1. University of Trento, Trento, Italy.

Open Access Funding provided by Universita degli Studi di Trento within the CRUI-CARE Agreement.

WOA Institution: Universita degli Studi di Trento
Consortia Name: CARE

2 Fragility methods and ground motion selection

2.1 Formulation of fragility models

Numerical simulations were performed by exploiting the Incremental Dynamic Analysis (IDA) [6] on finite element models built in OpenSees [5]. The structures were subjected to a suite of representative ground motion records, that were scaled to multiple levels of intensity. In order to reduce the computational burden, the maximum value of intensity was defined when either a maximum interstorey drift ratio of 5% or a maximum value of intensity was attained. The former can be associated to the collapse of the structure, according to FEMA356 for moment resisting frames [7], whilst the latter was defined by preliminary analyses performed to have a sufficient number m(<n) of ground motions entailing a structural collapse. In addition, to avoid numerical divergence occurring for low levels of intensity, Δt of each record was reduced up to a minimum value of 0.0005s.

From each ground motion, a different IDA curve was obtained, which relates an intensity measure (IM) to an engineering demand parameter (EDP). As discussed by Vamvastikos and Cornell [6] the intensity measure should be a non-negative scalar, monotonically increasing with the scaling factor that is employed for the records. Among many intensity measures, the spectral acceleration at the first mode of vibration period (Sa_{T1}) in the direction of the frame was selected. Moreover, Vamvastikos and Cornell [6] define a damage measure (or Engineering Demand Parameter) as a non-negative scalar that characterizes the additional response of the structural model due to a prescribed seismic loading. Hence, the Peak Interstorey Drift Ratio was regarded to be the damage measure that better represents the structural response in global terms.

After performing an IDA, fragility functions can be estimated for different levels of EDP, that can be identified with specific limit states, and can be used for a seismic risk assessment. The procedure followed to build the fragility functions is the one described by Baker [8], in which the basic assumption is that an intensity measure IM causing the exceedance of a limit state, identified as C, follows a lognormal cumulative distribution function, of the form:

$$P(C|IM = x) = \Phi\left(\frac{\ln(x/\theta)}{\beta}\right) \quad (1)$$

where $\Phi()$ is the standard normal cumulative distribution function (CDF), θ is the median of the fragility function and β is the standard deviation of ln(IM). After performing IDA for a set of n accelerograms, a set of IMs associated with the onset of collapse is obtained. In the case that all the records lead to structural collapse within the maximum IM value, estimations of θ and β are obtained from this set of IM, assuming it to be lognormally distributed:

$$\ln(\hat{\theta}) = \frac{1}{n}\sum_{i=1}^{n} \ln IM_i \quad (2)$$

$$\hat{\beta} = \sqrt{\frac{1}{n-1}\sum_{i=1}^{n}(\ln(IM_i/\hat{\theta})^2} \quad (3)$$

As previously described, several analyses were performed up to a predetermined value of IM, were just $m(<n)$ ground motions cause the surpass of the limit state. The remaining n-m records do not provide sufficient data for estimating fragility functions according to the previous equations. For such records instead, the maximum likelihood method is employed to extrapolate the fragility functions parameters. The likelihood function of the entire dataset is obtained by assuming that all the n values of IM for each ground motion are independent between each other. Thus, considering both the likelihood function of the m ground motions that cause collapse, and the likelihood function of the n-m ground motions that do not cause collapse at the maximum value of IM, the likelihood function of the entire data set is defined as:

$$Likelihood = \left(\prod_{i=1}^{m} \phi\left(\frac{\ln(IM_i/\theta)}{\beta}\right)\right)\left(1 - \boldsymbol{\Phi}\left(\frac{\ln(IM_{max}/\theta)}{\beta}\right)\right)^{n-m} \quad (4)$$

where the function variables are the fragility functions parameters θ and β. Such function gives an estimation of how likely an arbitrary couple of values (θ, β) is to well represent the set IM_i given as input. In general, the estimations of θ and β can be obtained by maximizing the likelihood function. Maximizing the logarithm of the likelihood function results to be a mathematically equivalent procedure, given the monotonicity of the logarithm function, yet numerically easier. Therefore, the parameters estimation is obtained by finding the couple of parameters that maximize the logarithm of the likelihood function:

$$\{\hat{\theta}, \hat{\beta}\} = \arg\max_{\theta,\beta} \sum_{j=1}^{m}\left\{\ln\phi\left(\frac{\ln(IM_i/\theta)}{\beta}\right)\right\} + (n-m)\ln\left(1 - \Phi\left(\frac{\ln(IM_{max}/\theta)}{\beta}\right)\right) \quad (5)$$

Finally, an estimation of the cumulative distribution function of the IM for which a certain threshold of collapse is exceeded, i.e. the fragility curve, can be represented by a lognormal distribution whose parameters are $\hat{\theta}$ and $\hat{\beta}$.

2.2 Selection of ground motions

A set of 20 accelerograms were used to perform the IDAs and selected from the NGA-West2 PEER database [9] as well as the corresponding European database ESM of ORFEUS [10]. Near-field and far-field accelerograms were chosen, considering a Joyner-Boore distance (R_{jb}) of less than 30 km. Moreover, pulse-like records [10] were also selected to have a comprehensive description of all the possible cases. A Consequence class of CC2 and a site category A according to [11] were chosen as they are consistent with the ones used to define the response spectrum for designing the structures. The acceleration spectrum obtained considering a damping ratio of 2% is reported in Figure 1.

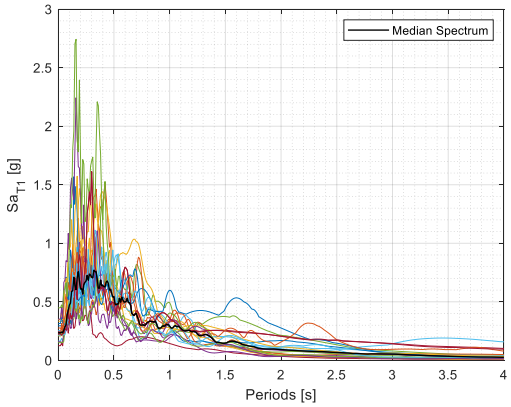

Figure 1 Response spectra of the selected records (ζ = 2%)

Table 1 Time History Search Parameters

N°	Database Record Number	Com ponent	Event	Year	M_w
1	A.487	East	Duzce, Turkey	1999	7.3
2	A.498	East			
3	E.SRC0	East	Friuli, 3rd shock	1976	6.0
4	EU.ULA	East	North-western Balkan Peninsula	1979	6.9
5		North			
6	IT.MRM	East	Cosenza	2012	5.2
7	IV.EVRN	East	Sicily Italy	2018	4.9
8	IV.T1212	North	Central Italy	2016	6.5
9	KO.GMLD	North	Dodecanese Islands, Greece	2020	7.0
10	TK.4101	East	Izmit, Turkey	1999	7.6
11	RSN 763	North	Loma Prieta	1989	6.93
12	RSN 809	North			
13	RSN 810	East			
14	RSN 989	North	North ridge 1st shock	1994	6.69
15	RSN 1011	East			
16	RSN 1091	East			
17	RSN 1161	East	Kocaeli, Turkey	1999	7.51
18	RSN 1165	North			
19	RSN 4483	East	L'Aquila, Italy	2009	6.3
20	RSN 5618	North	Iwate, Japan	2008	6.9

3 Numerical modelling of the case studies

The two-dimensional model of the state-of-the-art frame as well as the DISSIPABLE frames were designed based on three-dimensional buildings with the same geometric characteristics, as shown for one of them in Figure 2. The structures had two spans in the transverse direction and three in the longitudinal direction. The spans were set at 4.275m in both directions while the storey height was 3.5m. In the three models, a braced system was design to withstand horizontal actions in the longitudinal direction. The three models differ in terms of the structural system in the transverse direction: moment-resisting frames were employed for the state-of-the-art building, whilst DRLF system and DRBeS components were considered for DISSIPABLE structures. For the moment resisting frame and the frame equipped with DRBeS devices, all frames placed in the transverse direction were considered seismic-resistant, while for the DRLF frame, only the external frames were responsible for resisting horizontal actions.

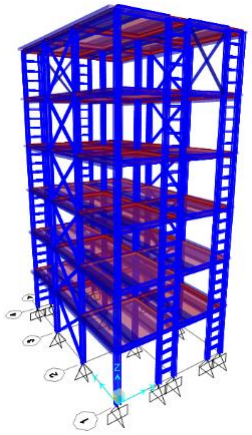

Figure 2 DRLF – 3D Building

3.1 State of the art model

The moment resisting frame was designed according to Eurocode 8 [11] provisions by means of linear dynamic analysis. The structure is a six-storey frame with two spans, as depicted in Figure 3. As previously illustrated, the geometry of the frame was chosen to be the same of the DISSIPABLE structure, leading, as shown in Table 2, to different dynamic characteristics from the previous structures. The non-linear behaviour of the structure was modelled by means of fibre elements for both columns and composite beams, in particular, fiber elements describing the spread of plasticity were preferred to concentrated plasticity models capable of capturing the non-linear buckling behaviour since preliminary analyses performed according to [13] showed that no significant buckling effects developed in the steel beams. For this frame, Rayleigh damping on the first and third mode and a damping ratio of 5%, as suggested by [9] for bolted steel structures, were employed. For DISSIPABLE structures conversely the damping ratio was set to 2% since lower viscous damping is expected for a structure with dissipative components with respect to one designed according to the capacity design.

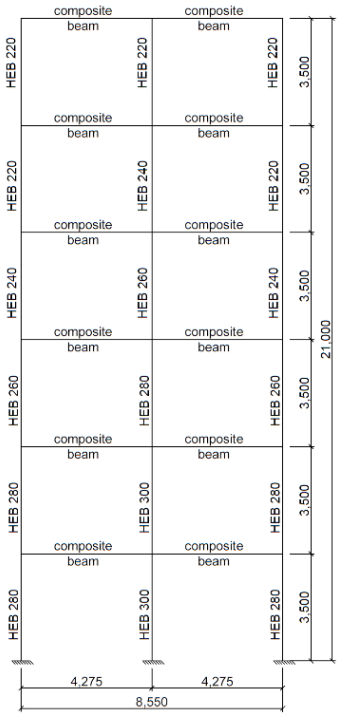

Figure 3 State-of-the-art building

Table 2 State-of-the-art vibration periods

Mode	Periods [s]
1	1.08
2	0.36
3	0.21

3.2 DRLF model

The Dissipative Replaceable Link Frame system shown in Figure 4 is conceived to be placed in the external frames of a steel building. The component is made up of two parallel strong columns connected by beam links with weakened sections at both ends [14].

Figure 4 DRLF system configuration

The IDAs for the DRLF system were performed on a six-storey frame with two spans, as for the frame experimentally tested, and depicted in Figure 5. For this frame, the non-linearity was concentrated at the reduced beam sections (RBSs) and modelled by means of piece-wise model namely "modified Ibarra-Krawinkler deterioration model with bilinear hysteretic response" [15], whose parameters were analytically determined. Those parameters were found to be in accordance with the results of the experimental campaign at the University of Trento. Beams and braces were modelled with elastic elements, since buckling effects as well as plasticity did not occur, whilst fibre-elements were employed for the columns, to account for plasticity and to detect the column-base yielding. The modal characteristics of the structure are listed in Table 3.

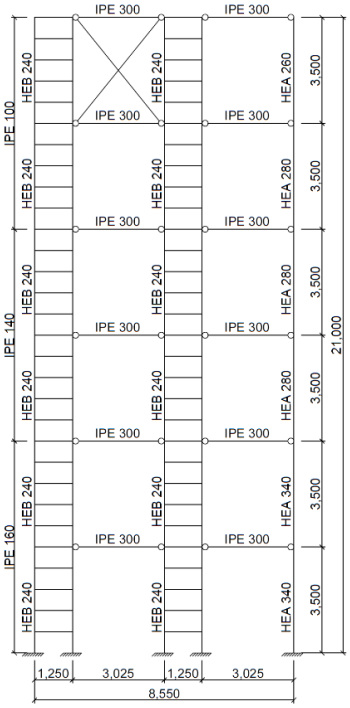

Figure 5 DRLF building

Table 3 DRLF vibration periods

Mode	Periods [s]
1	1.38
2	0.35
3	0.19

3.3 DRBeS model

The Dissipative Replaceable Beam Splice was designed for moment resisting frames, with the purpose of weakening the composite beam and localise the plastic hinges close to the beam column joint. This was achieved by interrupting the steel profile and the concrete slab, as shown in Figure 6, and restoring the continuity with fuse plates on the web and the flange of the steel profile, the latter were designed to dissipate energy [16].

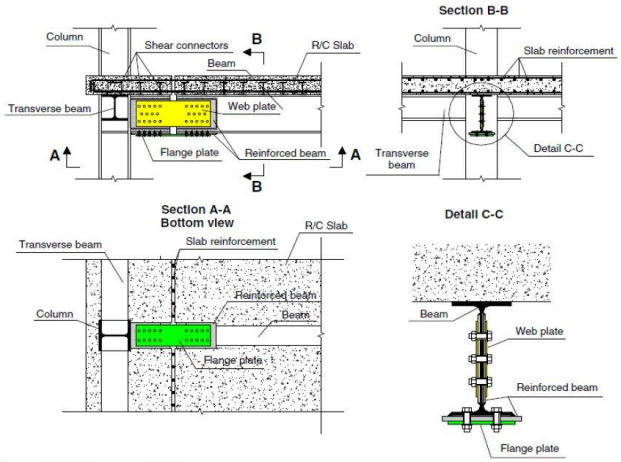

Figure 6 Front, lateral and plan view of DRBeS

The frame under investigation is a six-storey frame with two spans as depicted in Figure 7, like the frame experimentally tested, equipped with DRBeS devices [14]. OpenSees was used to model the frame. The INNOSEIS provisions [14] were followed to model the constitutive relationship of the DRBeS components. The columns were instead modelled as fibre sections elements, in order to be able to detect possible yielding at their base. The modal properties of the structure are listed in the table below.

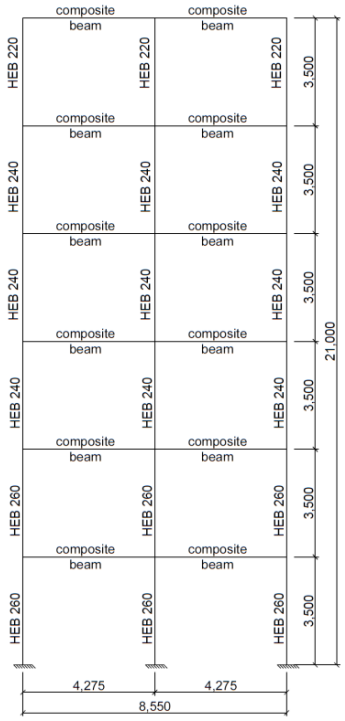

Figure 7 DRBeS building

Table 4 DRBeS - vibration periods

Mode	Periods [s]
1	1.35
2	0.55
3	0.25

4 Seismic performance

4.1 Definition of the limit states

In order to assess the behaviour of the structures, two significant values of Peak Interstorey Drift Ratio (PIDR) are considered:

1. Peak Interstorey Drift Ratio equal to the median value for which the first column base section reaches the yielding of the outer fibers, which is different for each structure.

2. Peak Interstorey Drift Ratio equal to 5.0%, that is conventionally defined as the NC limit state threshold according to FEMA356 for moment resisting frames [7].

The performance levels are defined as the exceeding of aforementioned PIDRs which represents the so-called *EDP-based rule* [6] i.e. the EDP is the damage indicator whose value determine in which limit state the structural model is. Hence, these values were also considered to evaluate the fragility curves.

4.2 Probabilistic seismic demand analysis through IDAs

In this paragraph the results of IDAs are reported with the respect to the first period spectral acceleration (Sa_{T1}) which was chosen as Intensity Measure (*IM*) (Figure 8). IDAs results were additionally post processed to obtain capacity curves by plotting for each intensity measure the maximum top floor displacement versus the maximum base shear (Figure 9). These graphs were superimposed with the results of static non-linear analysis in order to compare the static and dynamic proprieties. In detail, pushover analyses were performed by means of lateral load distribution given by:

$$\overline{\boldsymbol{F_i}} = \boldsymbol{m_i} \cdot \overline{\boldsymbol{\Phi_i}} \qquad (6)$$

Where m_i is the mass of the i-th node whilst $\overline{\Phi_i}$ is the normalized mode of vibration that corresponds to the largest value of the effective modal mass, as defined by [11].

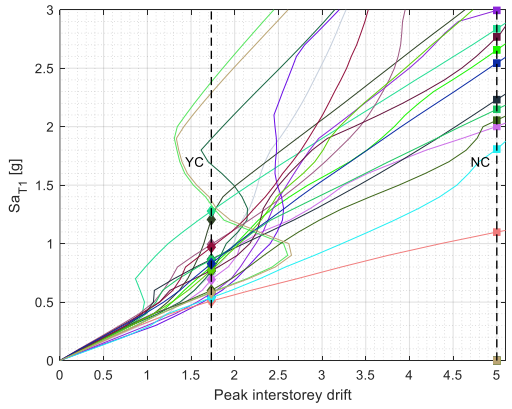

a)

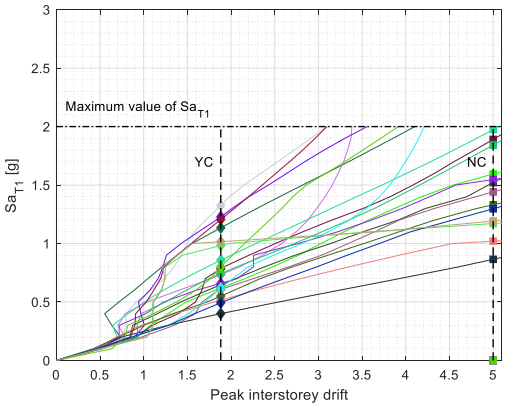

b)

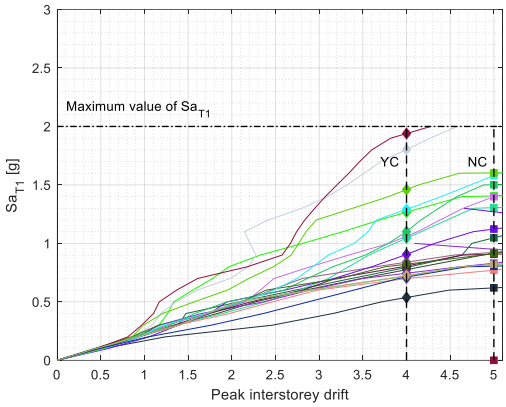

c)

Figure 8 IDA curves of a) SoA, b) DRLF and c) DRBeS Frames

From Figure 8, it may be noted that the maximum IM value chosen for the SoA structure is 3g otherwise for the DISSIPABLE buildings is equal to 2g. Different maximum IM values were chosen due to the higher stiffness of the moment resisting frame which needs stronger inputs to provide the same displacement value. Indeed, using a maximum IM value of 2g also for the SoA frame, the number of accelerograms leading to the collapse of the structure would not have been sufficient to derive a reliable fragility curve. From Figure 8a can be highlighted that, since the EDP-based rule is used, given a unique value of EDP threshold, multiple limit-state point on an IDA curve can be identified. This was handled by conservatively considering the lowest value of IM. In Figure 8b the IDAs curves of DRLF frame were reported. It can be highlighted that, for Sa_{T1}<0.2g, the structure is in the elastic range and the data have low variability. Instead, the higher dispersion of the results for Sa_{T1}>0.2g is due to the characteristics of the system. Indeed, compared with the other frames, the DRLF system presents the highest number of devices and owing to the progressive plasticisation of such devices, the dynamic characteristics of the frame change during a seismic event. Moreover, since each accelerogram may excite different vibration modes, the order in which the devices plasticise may vary as well, leading time to time to a different structural response. Same consideration for value of Sa_{T1} lower than 0.2g can be drawn from Figure 8c, whereas for Sa_{T1}>0.2g DRBeS frame results present lower dispersion because of the lower number of dissipative components.

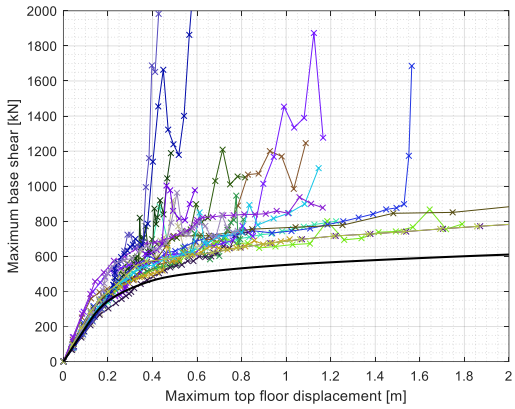

a)

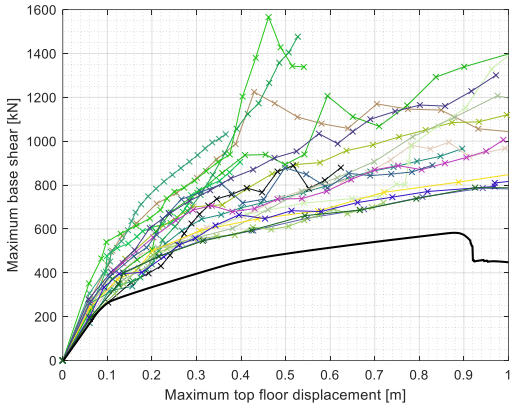

b)

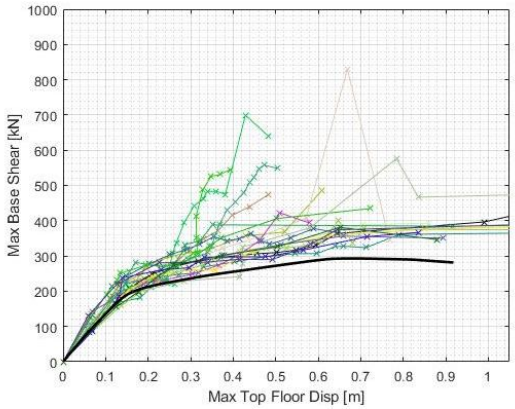

c)

Figure 9 Capacity curves of a) SoA, b) DRLF and c) DRBeS Frames

Figure 9a depicts the capacity curves of the SoA frame in comparison with the non-linear static curve. It can be observed that initial elastic stiffness estimated with the push-over analysis corresponds with the dynamic ones whilst IDAs show a different non-linear behaviour allowing for higher base shear values. Considering Figure 9b, it can be noticed that by means of a dynamic analysis, a difference between the dynamic capacity curves and the push-over one can be found for the DRLF frame given that high modes contribution, which is neglected from push-over analysis, is considered in non-linear dynamic analyses. In Figure 9c, it can be highlighted that, despite an initial correspondence between the static and dynamic curves, for high value of displacement of the top floor, the DRBeS frame shows higher values of base shear for the incremental dynamic analyses.

4.3 Fragility functions

In this paragraph, the fragility curves for the three previously illustrated frames are shown. Firstly, from all figures it can be deduced that the probability determined analytically, according to

the procedure illustrated above, well reproduces the distribution of the data for both limit states. In addition, the maximum IM value used in the analyses is shown for all the structures, i.e. 2g for the DISSIPABLE structures and 3g for the SoA building.

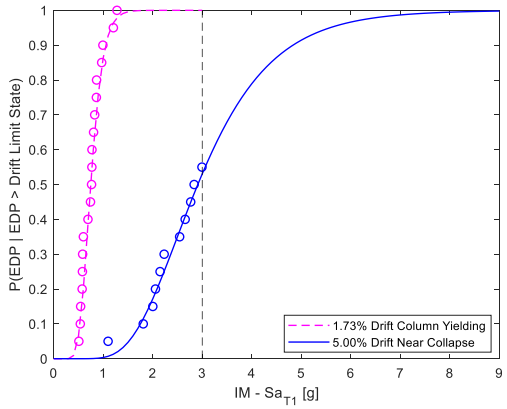

Figure 10 SoA building - Fragility Curves for limit states

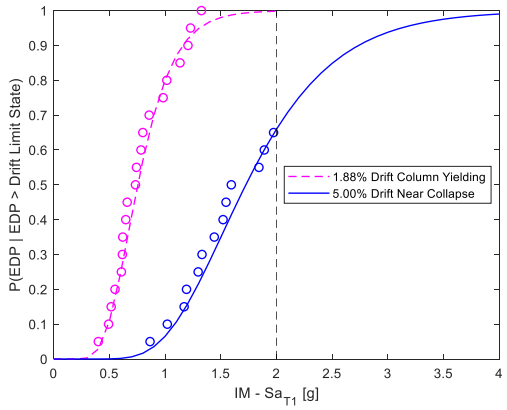

Figure 11 DRLF building - Fragility Curves for limit states

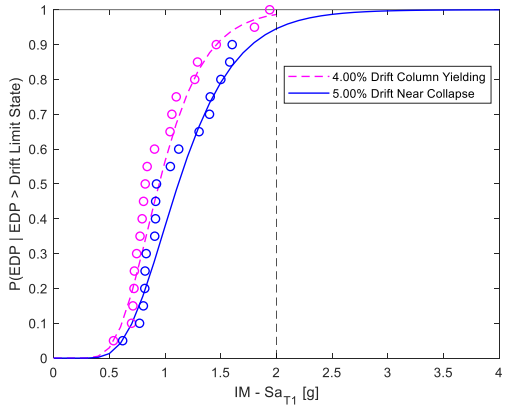

Figure 12 DRBeS building - Fragility Curves for limit states

5 Discussion of the results

Hereafter the comparison between the results obtained from the analyses on the three different structures is described. By comparing the dynamic characteristics, despite the three structures having the same geometry, the first period of the SoA structure is 22% lower than that of the DISSIPABLE structures, as can be seen from Table 2, Table 3 and Table 4. Furthermore, the structures were designed under the same gravity and seismic loads, therefore a lower first period involves that the SoA frame is stiffer than the others. In Figure 13 the comparisons in terms of fragility curves at near collapse limit state and at the mean peak interstorey drift are reported. Concerning Figure 13a which describes the probability of exceedance of the Peak Interstorey Drift Ratio for which the first yielding of the column base occurs, the DRBeS frame has the lowest probability of exceedance, which is a favourable output of the research since the repairability of the structure should be guaranteed. It can also be highlighted that for an EDP limit value related to a physical phenomenon such as the column base yielding, the DRBeS frame has a lower probability of exceedance compared to the other structures, in countertendency to the fragility curves related to the conventional EDP threshold values. On the contrary, as depicted in Figure 13b, which represents the fragility curves at the near collapse limit state, the DRBeS frame has the highest probability of reaching a near collapse limit state at the same level of spectral acceleration.

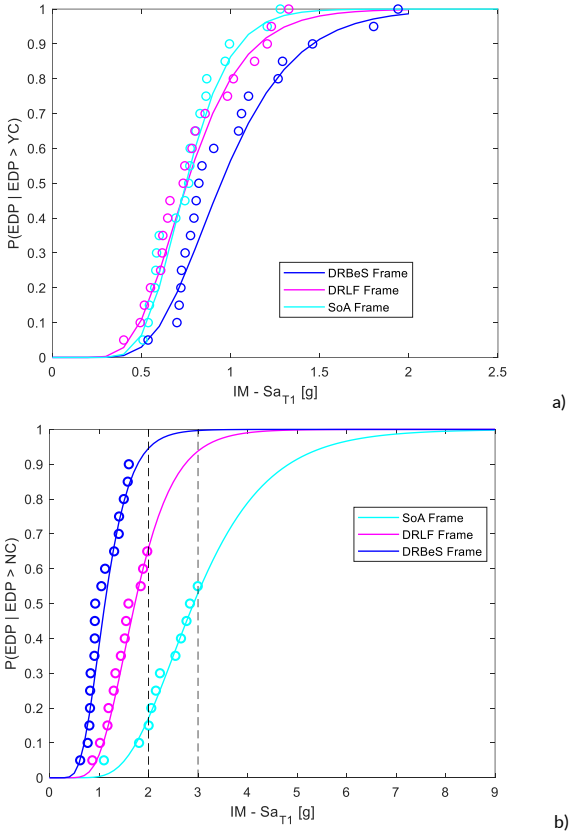

Figure 13 Fragility curves comparison at significant Peak Interstorey Drift Ratio

In Figure 14 and Figure 15 the overlapping of the IDA curves and capacity curves for the three structures are respectively reported. In both cases, the percentiles 16, 50 and 84 were employed for the comparison as suggested in [6]. For both Figure 14 and Figure 15 it has been decided not to consider the results of the analysis of DRBeS frame with Sa_{T1} greater than 0.9g, since the collapse threshold of 5% of interstorey drift was already reached in most of the analyses. From both Figure 14 and Figure 15 it can be highlighted that DRBeS and DRLF frames had a similar initial stiffness, as it can also be noted from the first period of the two structures. However, after the first yields occur, the DRLF system preserved greater stiffness, due to the highest number of dissipative devices.

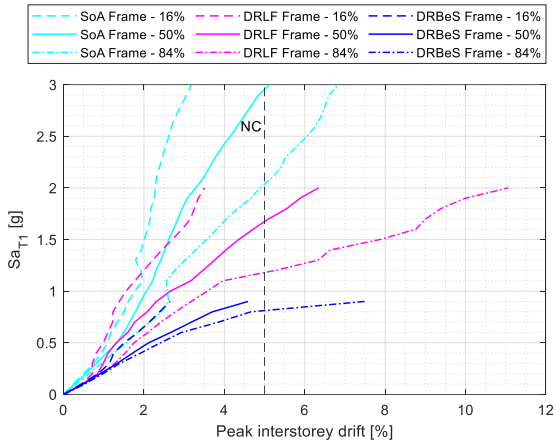

Figure 14 IDA curves comparison between SoA Frame ad DISSIPABLE Frames

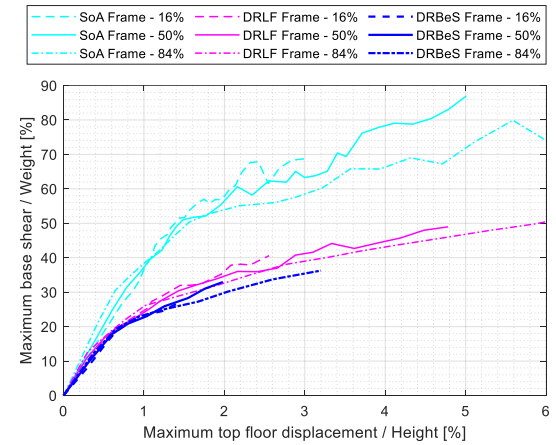

Figure 15 Capacity curves comparison between SoA Frame ad DISSIPABLE Frames

6 Conclusions

The paper has presented a probabilistic seismic demand analysis of bi-dimensional frames with dissipative components. Specifically, Incremental Dynamic Analyses were performed in order to assess the structural behaviour of structures equipped with DRBeS components and DRLF systems. The structural response of the two frames has been compared with a conventional moment resisting frame, namely State-of-the-Art building. The seismic performances were investigated by means of a nonlinear FE model built in OpenSees and calibrated on experimental data. For DRBeS frame, favourable outcomes were deduced in terms of structural performance, since yielding of the base column occurred after the Significant Damage limit state and the columns are consequently protected for a seismic event corresponding to such limit state. This validates the effective repairability of the frame for the limit state to which the building was designed for. The DRLF system exhibited a high deformation capacity, comparable with the one of the reference model. As the intensity measure increases, the DRLF system also retained a high stiffness due to the elevated number of devices.

In future developments, the fragility curves at different limit state should be derived and different EDP, e.g. the deformation of the dissipative components or the residual interstorey drift, could be considered to thoroughly investigate the benefit of equipping steel frames with DISSIPABLE components.

7 Acknowledgements

This work was carried out with a financial grant from the Research Fund for Coal and Steel of the European Union, within the DISSIPABLE project: "Fully dissipative and easily repairable devices for resilient buildings with composite steel-concrete structures", Grant No. 800699-RFCS-2017.

The support received from the Italian Ministry of Education, University and Research (MIUR) in the frame of the 'Departments of Excellence' (grant L 232/2016) is gratefully acknowledged.

Acknowledgements should be given to the National Technical University of Athens (NTUA) as well, in the person of Lydia Panoutsopoulou, for her support in the selection of the accelerograms.

References

[1] Tondini, N., Zanon, G., Pucinotti, R., di Filippo, R. & Bursi, O.S. (2018). Seismic performance and fragility functions of a 3D steel-concrete composite structure made of high-strength steel. *Engineering Structures 174, 373–383.* https://doi.org/10.1016/j.engstruct.2018.07.026

[2] Nam Phan, H., Paolacci, F., Bursi, O.S. & Tondini, N. (2017). Seismic fragility analysis of elevated steel storage tanks supported by reinforced concrete columns. *Journal of Loss Prevention in the Process Industries 47, 57-65.* http://dx.doi.org/10.1016/j.jlp.2017.02.017

[3] Abbiati, G., Broccardo, M., di Filippo, R., Stojadinović, B., & Bursi, O.S. (2021). Seismic fragility analysis of a coupled tank-piping system based on artificial ground motions and surrogate modelling. *Journal of Loss Prevention in the Process Industries 72, 104575.* https://doi.org/10.1016/j.jlp.2021.104575

[4] CSI, "SAP2000 Integrated Software for Structural Analysis and Design" Computers and Structures Inc., Berkeley, California.

[5] OpenSees. https://opensees.berkeley.edu/.

[6] Vamvatsikos, D., & Cornell, C. A. (2002). Incremental dynamic analysis. *Earthquake engineering & structural dynamics*, *31*(3*), 491-514.* https://doi.org/10.1002/eqe.141

[7] FEMA 356 (2000). Prestandard and Commentary for the Seismic Rehabilitation of Buildings. Washington DC.

[8] Baker, J. W. (2015). Efficient analytical fragility function fitting using dynamic structural analysis. *Earthquake Spectra, 31(1), 579-599.*

[9] PEER Ground Motion Database, https://ngawest2.berkeley.edu/

[10] Luzi L., Puglia R., Russo E & ORFEUS WG5 (2016). Engineering Strong Motion Database, version 1.0. Istituto Nazionale di Geofisica e Vulcanologia, Observatories & Research Facilities for European Seismology. doi: 10.13127/ESM https://esm.mi.ingv.it/

[11] Eurocode 8: Design of structures for earthquake resistance. 1998.

[12] Chopra, A. K. (2007). *Dynamics of structures: Theory and applications to earthquake engineering*. Upper Saddle River, N.J: Pearson/Prentice Hall. ISBN 10: 0132858037

[13] Pecce, M., & Rossi, F. (2015). The experimental behavior and simple modeling of joints in composite MRFs. *Engineering Structures*, *105*, 249-263. https://doi.org/10.1016/j.engstruct.2015.09.042

[14] Research Fund for Coal and Steel INNOSEIS Project RFCS-02-2015 (2017): Innovative anti-seismic components and systems. ECCS – European Convention for Constructional Steelwork.

[15] Lignos, D. G., & Krawinkler, H. (2007). A database in support of modeling of component deterioration for collapse prediction of steel frame structures. In *Structural Engineering Research Frontiers* (pp. 1-12). https://doi.org/10.1061/40944(249)31

[16] Kanyilmaz, A., Muhaxheri, M., & Castiglioni, C. A. (2019). Influence of repairable bolted dissipative beam splices (structural fuses) on reducing the seismic vulnerability of steel-concrete composite frames. *Soil Dynamics and Earthquake Engineering*, *119*, 281-298. https://doi.org/10.1016/j.soildyn.2019.01.007